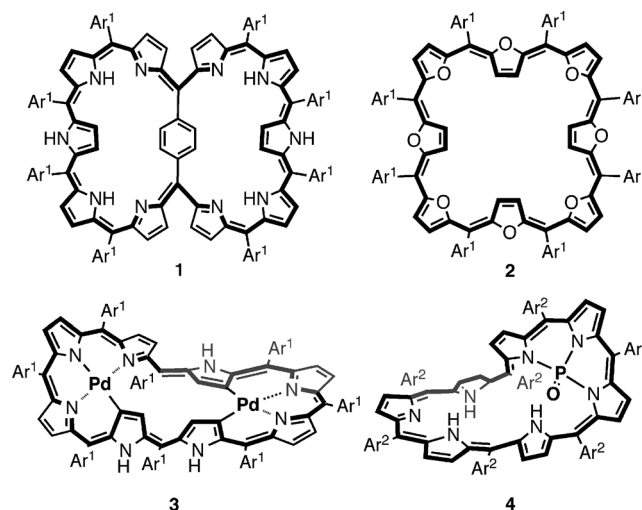


# Pd<sup>II</sup> Complexes of [44]- and [46]Decaphyrins: The Largest Hückel Aromatic and Antiaromatic, and Möbius Aromatic Macrocycles\*\*

Tomoki Yoneda, Young Mo Sung, Jong Min Lim, Dongho Kim,\* and Atsuhiko Osuka\*

**Abstract:** Reductive metalation of [44]decaphyrin with [Pd<sub>2</sub>(dba)<sub>3</sub>] provided a Hückel aromatic [46]decaphyrin Pd<sup>II</sup> complex, which was readily oxidized upon treatment with DDQ to produce a Hückel antiaromatic [44]decaphyrin Pd<sup>II</sup> complex. In CH<sub>2</sub>Cl<sub>2</sub> solution the latter complex underwent slow tautomerization to a Möbius aromatic [44]decaphyrin Pd<sup>II</sup> complex which exists as a mixture of conformers in dynamic equilibrium. To the best of our knowledge, these three Pd<sup>II</sup> complexes represent the largest Hückel aromatic, Hückel antiaromatic, and Möbius aromatic complexes to date.

Recent progress in the chemistry of expanded porphyrins has covered a diverse range of interesting topics such as their rich coordination behavior, large nonlinear optical properties, multistep reversible redox responses, and unprecedented characteristic chemical reactions.<sup>[1]</sup> In addition, regarding their flexible electronic properties, expanded porphyrins may be either Hückel aromatic, Hückel antiaromatic,<sup>[2]</sup> Möbius aromatic,<sup>[3]</sup> or Möbius antiaromatic,<sup>[4]</sup> depending upon the number of π-electrons and the molecular topology. As an intriguing attribute, expanded porphyrins are known to realize large aromatic or antiaromatic species. In fact, internally 1,4-phenylene-bridged [46]decaphyrin **1**<sup>[5a,6]</sup> and core-modified [40]octaphyrin **2**<sup>[5b]</sup> represent, to the best of our knowledge, the largest Hückel aromatic and antiaromatic molecules, respectively. On the other hand, the bis-Pd<sup>II</sup> [36]octaphyrin complex **3**<sup>[3b]</sup> and phosphorus [34]heptaphyrin complex **4**<sup>[4c]</sup> are respectively the largest Möbius aromatic and antiaromatic molecules to date (Scheme 1). It is an important synthetic challenge to explore aromatic and antiaromatic molecules that surpass the sizes of conventional examples. A simple yet promising strategy may be to employ expanded



**Scheme 1.** Hückel aromatic **1**, Hückel antiaromatic **2**, Möbius aromatic expanded porphyrin **3**, and Möbius antiaromatic expanded porphyrin **4** (Ar<sup>1</sup> = C<sub>6</sub>F<sub>5</sub>, Ar<sup>2</sup> = 2,6-dichlorophenyl). Their conjugate circuits are indicated in bold.

porphyrins<sup>[7]</sup> as a macrocyclic platform, but conformational and electronic control of expanded porphyrins becomes increasingly difficult with increasing ring size, due to inherent conformational deviation from planarity and chemical instability associated with small HOMO–LUMO band gaps. In the cases of **1**, **3**, and **4**, the 1,4-phenylene bridge, palladium coordination, and phosphorus insertion serve to rigidify the overall conformations.

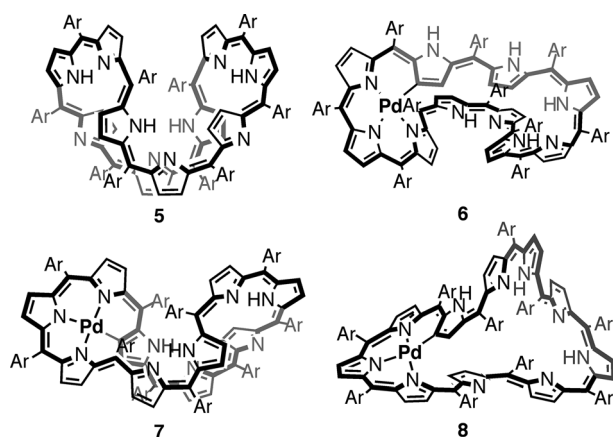
[44]Decaphyrin **5** is a large expanded porphyrin that can be prepared from the condensation reaction of *meso*-pentafluorophenyl-substituted dipyrromethane with pentafluorobenzaldehyde.<sup>[7i]</sup> The solid-state structure of decaphyrin **5** has been revealed to be a crescent shape and its nonaromatic nature is indicated by its <sup>1</sup>H NMR spectrum,<sup>[7i]</sup> but its chemistry has been left almost unexplored due to limited synthetic access. In addition, the large cyclic conjugated electronic network and chemical stability are attributes that make **5** an attractive platform for constructing large exotic aromatic systems. In this paper, we report Pd<sup>II</sup> metalation of **5**, which led to the formation of [46]decaphyrin Pd<sup>II</sup> complex **6** and [44]decaphyrin Pd<sup>II</sup> complexes **7** and **8** (Scheme 2). Importantly, these complexes are the largest untwisted Hückel aromatic, doubly twisted Hückel antiaromatic, and singly twisted Möbius aromatic molecules, respectively.

After extensive screening of reaction conditions, complex **6** was synthesized in 55% yield by treating **5** with [Pd<sub>2</sub>(dba)<sub>3</sub>] (dba = 1,5-diphenyl-1,4-pentadien-3-one) in the presence of

[\*] T. Yoneda, Prof. Dr. A. Osuka  
Department of Chemistry, Graduate School of Science  
Kyoto University  
Sakyo-ku, Kyoto 606-8502 (Japan)  
E-mail: osuka@kuchem.kyoto-u.ac.jp  
Y. M. Sung, Dr. J. M. Lim, Prof. Dr. D. Kim  
Spectroscopy Laboratory for Functional π-Electronic Systems  
and Department of Chemistry, Yonsei University  
Seoul 120-749 (Korea)  
E-mail: dongho@yonsei.ac.kr

[\*\*] The work at Kyoto was supported by Grants-in-Aid (no. 22245006 (Scientific Research S) from JSPS and by MEXT. T.Y. acknowledges a JSPS Fellowship for Young Scientists. The work at Yonsei was supported by the Global Research Laboratory (GRL) Program (2013-8-1472) of the Ministry of Education, Science, and Technology (MEST) of Korea.

Supporting information for this article is available on the WWW under <http://dx.doi.org/10.1002/anie.201408506>.



**Scheme 2.** [44]Decaphyrin **5**, and decaphyrin Pd<sup>II</sup> complexes **6**, **7**, and **8** (Ar = C<sub>6</sub>F<sub>5</sub>). Their conjugate circuits are indicated in bold.

sodium acetate in a mixture of CH<sub>2</sub>Cl<sub>2</sub> and methanol. This reductive metalation led to a better yield than that of nonreductive metalations of [46]decaphyrin with Pd<sup>II</sup> salts.<sup>[8]</sup> This outcome is reminiscent of the successful synthesis of a [28]hexaphyrin Pd<sup>II</sup> complex from its corresponding [26]hexaphyrin free-base analogue.<sup>[9]</sup> The structure of **6** has been determined by X-ray crystallographic analysis. In **6** the Pd center is bound to the C3 carbon of pyrrole A and three pyrrolic nitrogen atoms of pyrroles B, C, and D with distances of 1.967(8), 1.988(7), 2.028(7), and 1.966(8) Å, or 1.950(8), 1.979(8), 2.037(8), and 1.959(8) Å, respectively, for the two slightly different structures in the asymmetric unit (Figure 1a).<sup>[10]</sup> According to the definition proposed by Latos-Grażyński et al.,<sup>[11e]</sup> **6** can be classified as an untwisted 70 ring conformer (Figure 1b). Importantly, the largest dihedral angle is only 29–32°, allowing smooth conjugation along the macrocycle. The <sup>1</sup>H NMR spectrum of **6** shows signals due to the inner pyrrolic β-protons in the pyrrole rings A and J at high field at δ = 2.45 and 4.38, and 3.00 ppm, indicating its

diatropic ring current. The conjugated network of **6** is comparable in size to that of the 1,4-phenylene-bridged [46]decaphyrin **1**.<sup>[5a,6]</sup> Macrocycle **1** showed sharp <sup>1</sup>H NMR signals only at low temperature while the <sup>1</sup>H NMR spectrum of **6** displayed sharp signals at room temperature, indicating that the conformation of **6** is more rigid than that of **1**. In line with the above presumption, the absorption spectrum of **6** displays a sharper and more intense Soret-like band at 863 nm in the near-infrared (NIR) region and more distinct Q-like bands at 939 and 1153 nm, indicating further that its aromatic character is stronger than that of **1** (Figure 2).

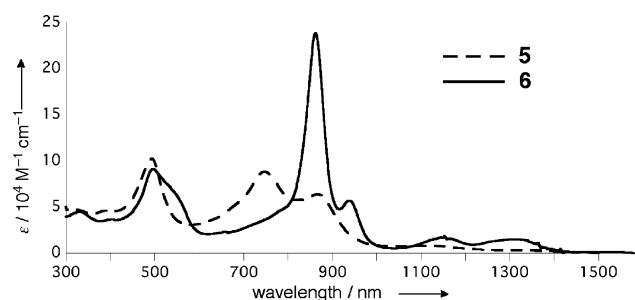


**Figure 2.** UV/Vis absorption spectra of **5** and **6** in CH<sub>2</sub>Cl<sub>2</sub>.

In the next step, quick oxidation of **6** with 2,3-dichloro-5,6-dicyano-1,4-benzoquinone (DDQ) produced the [44]decaphyrin Pd complex **7** in 61% yield as a green solid. The structure of **7** has been revealed by X-ray diffraction analysis to be a 360° twisted (figure-eight) crescent-like conformation (Figure 1c,d).<sup>[11]</sup> Therefore, complex **7** has been confirmed to possess a doubly twisted Hückel topology (*T*<sub>2</sub> ring conformer)<sup>[11e]</sup> with smooth conjugation characterized by a largest dihedral angle of 31°. The <sup>1</sup>H NMR spectrum of **7** shows signals due to the inner NH protons at δ = 16.56 ppm, 13.25 ppm, and 11.44 ppm, and signals due to the inner pyrrolic β-protons in the pyrrole rings A and I at δ = 10.56 and

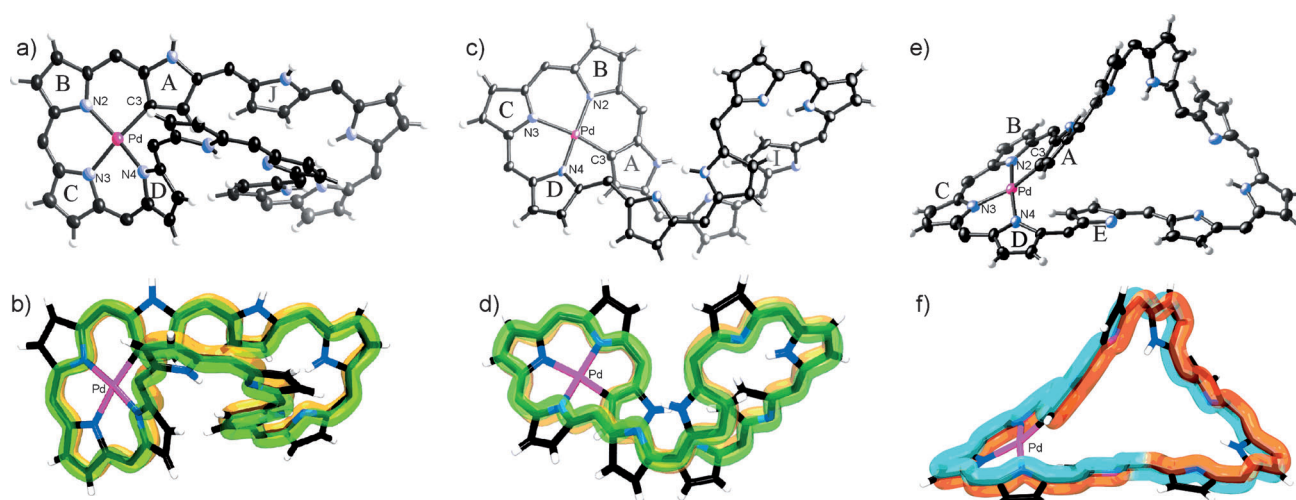


**Figure 1.** X-ray crystal structures of a) **6**, c) **7**, and e) **8** and their schematic representations of π-orbital of b) **6**, d) **7**, and f) **8**. *meso*-Pentafluorophenyl substituents and solvent molecules are omitted for clarity. The thermal ellipsoids are drawn at 30% probability level in (a), (c), and (e). One of two slightly different independent structures in the asymmetric unit is shown in (a) and (e).

10.23, and 9.17 ppm, while signals due to the outer nine  $\beta$ -protons appear in a range of  $\delta = 6.27$ – $5.67$  ppm, indicating a moderate paratropic ring current. The absorption spectrum of **7** shows an ill-defined Soret-like band at 733 nm along with weak and broad bands in the NIR region reaching ca. 1900 nm. These absorption features are characteristic of antiaromatic expanded porphyrins (Figure 3a and Figure S13). It should be noted that complex **7** is the largest Hückel antiaromatic molecule to date.

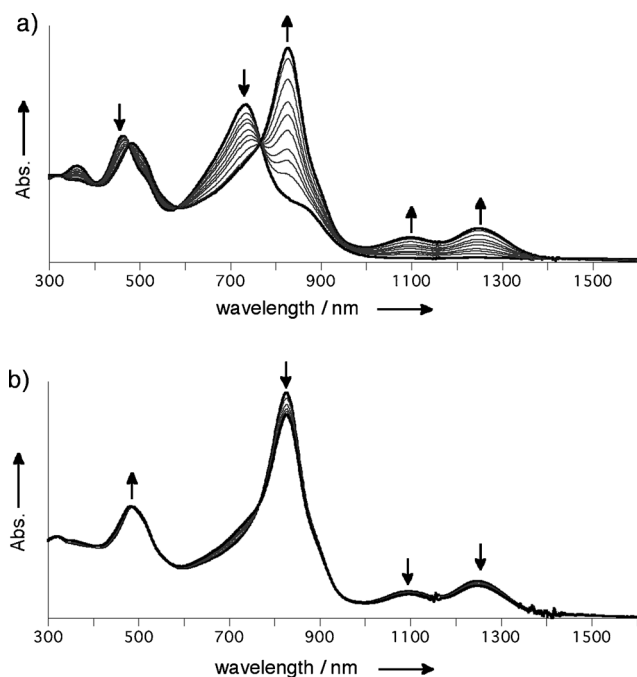


**Figure 3.** Time-dependent changes in the absorption spectra of a) **7** and b) **8** in  $\text{CH}_2\text{Cl}_2$ .

On standing, a green solution of **7** in  $\text{CH}_2\text{Cl}_2$  changed slowly to a deep brown solution. We monitored this change by  $^1\text{H}$  NMR and UV/Vis absorption spectroscopy and found that **7** isomerized to its tautomer with a different conformation, which has been assigned as **8** (Figure 3a). Somewhat serendipitously, we succeeded in preferential recrystallization of **8** by slow diffusion of heptane into a mixture of **7** and **8** in  $\text{CCl}_4$ . The structure of **8** has been revealed by X-ray diffraction analysis to assume a twisted Möbius conformation, which has one topological phase inversion (*TI* ring conformer)<sup>[1e]</sup> but its  $\pi$ -conjugation circuit is again relatively smooth (Figure 1e,f).<sup>[12]</sup> The  $^1\text{H}$  NMR spectrum of **8** shows signals due to the outer ten  $\beta$ -protons in the range of  $\delta = 8.29$ – $7.31$  ppm and those of the inner three  $\beta$ -protons in the pyrrole rings A and E at  $\delta = 4.32$  and 4.77, and 4.24 ppm, indicating its diatropic ring current, and hence Möbius aromatic nature for **8**. In line with this assignment, the UV/Vis absorption spectrum of **8** exhibits a sharp Soret-like band at 827 nm and Q-like bands at 1096 and 1298 nm as characteristic features of aromatic porphyrinoids. In the Möbius aromatic porphyrinoids reported so far, it is generally necessary to introduce a severely distorted site to effect a phase

change.<sup>[1e,3b]</sup> However, in **8**, despite its Möbius topology, the largest dihedral angles are only 23–24°, allowing relatively smooth conjugation. This favorable structural feature comes from its pseudo-triangular shape, whereby the three 180° contorted dipyrromethene units are located at the corners to accommodate not only a smooth cyclic conjugation but also 180° topological inversion (Figure 4). Very recently, a similar

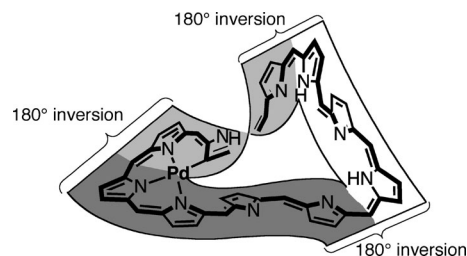


**Figure 4.** Schematic representation of the pseudo-triangle structure of **8** which consists of three relatively planar bands (indicated in white, light gray, and dark gray) connected by 180° written dipyrromethene corners.

triangle motif with 300° contorted 1,1'-dinaphthalene units was elegantly adopted in a triply twisted Möbius molecular system.<sup>[13]</sup> Complexes **7** and **8** interconverted slowly. Starting from a solution of either pure **7** or **8** in  $\text{CH}_2\text{Cl}_2$ , an equilibrium state was reached after ca. 8 h (see Figure 3). At equilibrium, the ratio of **7** and **8** was 1:6.5 at room temperature, indicating that **8** is more stable than **7** by 1.1 kcal mol<sup>-1</sup>.

Cyclic voltammetry (CV) measurements revealed reversible oxidation and reduction waves at 0.02 and  $-0.79$  V for **6**, at 0.40 and  $-0.38$  V for **7**, and at 0.41 and  $-0.50$  V for **8** versus a ferrocene/ferrocenium ion couple. The electrochemical HOMO–LUMO gaps are 0.81 eV for **6**, 0.78 eV for **7**, and 0.91 eV for **8**. The smaller HOMO–LUMO gap of **7** relative to that of **6** and **8** is consistent with its antiaromatic character. The HOMO–LUMO gaps estimated by their Q bands of UV/Vis absorption spectra are 0.91 eV for **6** and 0.95 eV for **8**, in good agreement with the electrochemical HOMO–LUMO gaps. The HOMO–LUMO gap estimated by the absorption end (1900 nm) of **7** is 0.65 eV, which is also consistent with the tendency.

To obtain further information, we performed DFT calculations on **6–8** (B3LYP/6-31G(d)/LANL2DZ)<sup>[14]</sup> (see the Supporting Information). These calculations revealed nearly degenerate HOMO/HOMO–1 and LUMO/LUMO+1 for **6** and **8** as characteristic features of aromatic porphyrins. The HOMO–LUMO gaps were calculated to be 1.33 and 1.27 eV for **6** and **8**, respectively. On the other hand, the calculated HOMO–LUMO gap of **7** was relatively small—only 0.98 eV. The nucleus-independent chemical shifts (NICS)<sup>[15]</sup> at the gravity points of the macrocycles were calculated to be  $-4.74$  and  $-9.53$  ppm for **6** and **8**, and the harmonic oscillator model of aromaticity (HOMA)<sup>[16]</sup> values of the optimized structures were calculated to be 0.61 and 0.62 for **6** and **8**. In contrast, the NICS and HOMA values of **7** were calculated to be  $+5.51$  ppm,<sup>[17]</sup> and 0.47, respectively, supporting the antiaromaticity of **7**.

We have investigated the excited-state dynamics of **6–8** by using femto-second transient absorption (fs-TA) spectroscopy (see the Supporting Information). In both aromatic and antiaromatic decaphyrin Pd<sup>II</sup> complexes, we observed long-lived transient species, which are usually not observed in their free-base congeners. These features can be explained in terms of the heavy-atom effect of the coordinated Pd centers, which accelerates intersystem crossing to populate the triplet states. Accordingly, we can assign the residual transient species remaining at longer time delay (ca. 3 ns) as the triplet excited state. Nevertheless, fs-TA results show distinct differences among the singlet excited-state dynamics of these complexes. The fs-TA spectra of **6–8** become complicated as the time delay changes due to distinct spectral changes arising from the intersystem crossing process. Thus, to distinguish the singlet excited-state dynamics from the intersystem crossing process and triplet excited-state dynamics, we have investigated the fs-TA decay dynamics in the NIR region where no spectral shift appears. In the case of antiaromatic **7**, the transient species reveals weak excited-state absorption (ESA) and ground-state bleaching (GSB) with double-exponential decay processes giving rise to two time constants of 0.5 and 4 ps with an additional residual component due to the triplet excited state. The fast time component of 0.5 ps seems to represent the internal conversion process from higher excited states to the lowest singlet excited state, and as a consequence a 4 ps decay component has been interpreted as a lifetime of the singlet excited state. We suggest that the relatively small HOMO–LUMO energy gap of **7** with the same symmetry of HOMO and LUMO produces a lower-lying energy dark state, which causes relatively fast internal conversion process.<sup>[18]</sup> In contrast to **7**, the excited-state dynamics of **6** and **8** exhibit single-exponential decay profiles with time components of 6 and 4 ps respectively. Overall, we have observed different excited-state dynamics of decaphyrin Pd<sup>II</sup> complexes depending on their aromatic/antiaromatic characteristics.<sup>[18]</sup>

In summary, the untwisted Hückel aromatic [46]decaphyrin **6**, the doubly twisted Hückel antiaromatic [44]decaphyrin **7**, and the singly twisted Möbius aromatic [44]decaphyrin **8** were synthesized from [44]decaphyrin **5**. The aromatic character of each has been confirmed on the basis of the respective X-ray structure, diatropic and paratropic ring currents, absorption characteristics, and excited-state dynamics. Möbius aromatic **8** has a triangle structure, which seems advantageous in achieving a smooth singly twisted molecular topology. Complexes **6**, **7**, and **8** represent the largest Hückel aromatic, Hückel antiaromatic, and Möbius aromatic molecules to date, respectively. In our research group we continue to actively explore larger aromatic and antiaromatic expanded porphyrins.

Received: August 25, 2014

Published online: September 24, 2014

**Keywords:** aromaticity · decaphyrins · Pd complexes · porphyrinoids · tautomerization

- [1] a) A. Jasat, D. Dolphin, *Chem. Rev.* **1997**, *97*, 2267; b) H. Furuta, H. Maeda, A. Osuka, *Chem. Commun.* **2002**, 1795; c) J. L. Sessler, D. Seidel, *Angew. Chem. Int. Ed.* **2003**, *42*, 5134; *Angew. Chem.* **2003**, *115*, 5292; d) T. K. Chandrashekar, S. Venkatraman, *Acc. Chem. Res.* **2003**, *36*, 676; e) M. Stępień, N. Sprutta, L. Latos-Grażyński, *Angew. Chem. Int. Ed.* **2011**, *50*, 4288; *Angew. Chem.* **2011**, *123*, 4376; f) S. Saito, A. Osuka, *Angew. Chem. Int. Ed.* **2011**, *50*, 4342; *Angew. Chem.* **2011**, *123*, 4432; g) A. Osuka, S. Saito, *Chem. Commun.* **2011**, 47, 4330.
- [2] a) S. Mori, A. Osuka, *J. Am. Chem. Soc.* **2005**, *127*, 8030; b) S. Mori, K. S. Kim, Z. S. Yoon, S. B. Noh, D. Kim, A. Osuka, *J. Am. Chem. Soc.* **2007**, *129*, 11344; c) K. Naoda, H. Mori, A. Osuka, *Chem. Asian J.* **2013**, *8*, 1395; d) H. Mori, Y. M. Sung, B. S. Lee, D. Kim, A. Osuka, *Angew. Chem. Int. Ed.* **2012**, *51*, 12459; *Angew. Chem.* **2012**, *124*, 12627.
- [3] a) M. Stępień, L. Latos-Grażyński, N. Sprutta, P. Chwalisz, L. Sztrenberg, *Angew. Chem. Int. Ed.* **2007**, *46*, 7869; *Angew. Chem.* **2007**, *119*, 8015; b) Y. Tanaka, S. Saito, S. Mori, N. Aratani, H. Shinokubo, N. Shibata, Y. Higuchi, Z. S. Yoon, K. S. Kim, S. B. Noh, J. K. Park, D. Kim, A. Osuka, *Angew. Chem. Int. Ed.* **2008**, *47*, 681; *Angew. Chem.* **2008**, *120*, 693; c) J. Sankar, S. Mori, S. Saito, H. Rath, M. Suzuki, Y. Inokuma, H. Shinokubo, K. S. Kim, Z. S. Yoon, J.-Y. Shin, J. M. Lim, Y. Matsuzaki, O. Matsushita, A. Muranaka, N. Kobayashi, D. Kim, A. Osuka, *J. Am. Chem. Soc.* **2008**, *130*, 13568; d) Z. S. Yoon, A. Osuka, D. Kim, *Nat. Chem.* **2009**, *1*, 113.
- [4] a) E. Pacholska-Dudziak, J. Skonieczny, M. Pawlicki, L. Sztrenberg, Z. Ciunik, L. Latos-Grażyński, *J. Am. Chem. Soc.* **2008**, *130*, 6182; b) T. Higashino, J. M. Lim, T. Miura, S. Saito, J.-Y. Shin, D. Kim, A. Osuka, *Angew. Chem. Int. Ed.* **2010**, *49*, 4950; *Angew. Chem.* **2010**, *122*, 5070; c) T. Higashino, B. S. Lee, J. M. Lim, D. Kim, A. Osuka, *Angew. Chem. Int. Ed.* **2012**, *51*, 13105; *Angew. Chem.* **2012**, *124*, 13282.
- [5] a) V. G. Anand, S. Saito, S. Shimizu, A. Osuka, *Angew. Chem. Int. Ed.* **2005**, *44*, 7244; *Angew. Chem.* **2005**, *117*, 7410; b) J. S. Reddy, S. Mandal, V. G. Anand, *Org. Lett.* **2006**, *8*, 5541.
- [6] In Ref. [1e], L. Latos-Grażyński et al. pointed out that the diatropic ring current of **1** has contributions from not only the 46π Hückel aromatic conjugation circuit, but also from two 28π Möbius aromatic *p*-benzihexaphyrin subrings. However, the contribution of the latter is inferred to be very small.
- [7] a) J.-i. Setsune, Y. Katakami, N. Iizuna, *J. Am. Chem. Soc.* **1999**, *121*, 8957; b) N. Sprutta, L. Latos-Grażyński, *Chem. Eur. J.* **2001**, *7*, 5099; c) J. L. Sessler, S. J. Weghorn, V. Lynch, M. R. Johnson, *Angew. Chem. Int. Ed. Engl.* **1994**, *33*, 1509; *Angew. Chem.* **1994**, *106*, 1572; d) R. Kumar, R. Misra, T. K. Chandrashekar, *Org. Lett.* **2006**, *8*, 4847; e) J.-i. Setsune, M. Toda, T. Yoshida, *Chem. Commun.* **2008**, 1425; f) J.-Y. Shin, H. Furuta, K. Yoza, S. Igarashi, A. Osuka, *J. Am. Chem. Soc.* **2001**, *123*, 7190; g) S. Shimizu, N. Aratani, A. Osuka, *Chem. Eur. J.* **2006**, *12*, 4909; h) S. Shimizu, W. S. Cho, J. L. Sessler, H. Shinokubo, A. Osuka, *Chem. Eur. J.* **2008**, *14*, 2668; i) Y. Tanaka, J.-Y. Shin, A. Osuka, *Eur. J. Org. Chem.* **2008**, 1341.
- [8] Formation of bis-Pd complex was not detected in the reductive Pd metalation.
- [9] T. Tanaka, T. Sugita, S. Tokuji, S. Saito, A. Osuka, *Angew. Chem. Int. Ed.* **2010**, *49*, 6619; *Angew. Chem.* **2010**, *122*, 6769.
- [10] Crystal data for **6**: (C<sub>110</sub>H<sub>24</sub>F<sub>30</sub>N<sub>10</sub>Pd)<sub>4</sub>·(C<sub>5</sub>(pentane))<sub>4</sub>·(O(water))<sub>2</sub> (*M*<sub>r</sub> = 5355.79), monoclinic, space group *P2<sub>1</sub>/n* (No. 14), *a* = 29.3092(5), *b* = 23.4512(4), *c* = 32.8397(6) Å, β = 102.1843(7)°, *V* = 22063.4(7) Å<sup>3</sup>, *Z* = 4, ρ<sub>calcd</sub> = 1.612 g cm<sup>-3</sup>, *T* = 93(2) K, *R*<sub>1</sub> = 0.1094 (*I* > 2σ(*I*)), *R*<sub>w2</sub> = 0.3583 (all data), GOF = 0.998, CCDC 1017503 contains the supplementary crystallographic data for this paper. These data can be obtained free of charge from The Cambridge Crystallographic Data Centre via [www.ccdc.cam.ac.uk/data\\_request/cif](http://www.ccdc.cam.ac.uk/data_request/cif).

- [11] Crystal data for **7**: (C<sub>110</sub>H<sub>22</sub>F<sub>50</sub>N<sub>10</sub>Pd<sub>1</sub>)(C<sub>5</sub>H<sub>12</sub>)<sub>2</sub> ( $M_r = 2684.07$ ), triclinic, space group  $P\bar{1}$  (No. 2),  $a = 12.961(5)$ ,  $b = 19.644(13)$ ,  $c = 22.332(16)$  Å,  $\alpha = 90.765(11)$ ,  $\beta = 100.12(4)$ ,  $\gamma = 95.80(3)^\circ$ ,  $V = 5566(7)$  Å<sup>3</sup>,  $Z = 2$ ,  $\rho_{\text{calcd}} = 1.602$  g cm<sup>-3</sup>,  $T = 93(2)$  K,  $R_1 = 0.0970$  ( $I > 2\sigma(I)$ ),  $R_{w2} = 0.2964$  (all data), GOF = 1.062, CCDC 1017504 contains the supplementary crystallographic data for this paper. These data can be obtained free of charge from The Cambridge Crystallographic Data Centre via [www.ccdc.cam.ac.uk/data\\_request/cif](http://www.ccdc.cam.ac.uk/data_request/cif).
- [12] Crystal data for **8**: (C<sub>110</sub>H<sub>22</sub>F<sub>50</sub>N<sub>10</sub>Pd<sub>1</sub>)(C<sub>7</sub>(heptane))<sub>6.5</sub> ( $M_r = 5626.01$ ), triclinic, space group  $P\bar{1}$  (No. 2),  $a = 21.668(5)$ ,  $b = 22.308(6)$ ,  $c = 27.100(6)$  Å,  $\alpha = 92.052(5)$ ,  $\beta = 90.379(9)$ ,  $\gamma = 108.316(7)^\circ$ ,  $V = 12425(5)$  Å<sup>3</sup>,  $Z = 2$ ,  $\rho_{\text{calcd}} = 1.504$  g cm<sup>-3</sup>,  $T = 93(2)$  K,  $R_1 = 0.1320$  ( $I > 2\sigma(I)$ ),  $R_{w2} = 0.4284$  (all data), GOF = 1.170, CCDC 1017505 contains the supplementary crystallographic data for this paper. These data can be obtained free of charge from The Cambridge Crystallographic Data Centre via [www.ccdc.cam.ac.uk/data\\_request/cif](http://www.ccdc.cam.ac.uk/data_request/cif).
- [13] G. R. Schaller, F. Topic, K. Rissanene, Y. Okamoto, J. Shen, R. Herges, *Nat. Chem.* **2014**, *6*, 608.
- [14] M. J. Frisch. et al., Gaussian09, revision A.02; Gaussian, Inc.: Wallingford, CT, **2009** (see the Supporting Information for the full citation).
- [15] a) P. v. R. Schleyer, C. Maerker, A. Dransfeld, H. Jiao, N. J. R. v. E. Hommes, *J. Am. Chem. Soc.* **1996**, *118*, 6317; b) Z. Chen, C. S. Wannere, C. Corminboeuf, R. T. Puchta, P. v. R. Schleyer, *Chem. Rev.* **2005**, *105*, 3842.
- [16] a) T. M. Krygowski, T. M. Cryański, *Tetrahedron* **1996**, *52*, 1713; b) T. M. Krygowski, T. M. Cryański, *Tetrahedron* **1996**, *52*, 10255.
- [17] In the NICS calculation of **7**, one pentafluorophenyl group was replaced by a hydrogen atom because the pentafluorophenyl group is in close proximity to the center of macrocycle.
- [18] S. Cho, Z. S. Yoon, K. S. Kim, M.-C. Yoon, D.-G. Cho, J. L. Sessler, D. Kim, *J. Phys. Chem. Lett.* **2010**, *1*, 89.